International Journal of Heat and Mass Transfer 52 (2009) 1864–1874

Contents lists available at ScienceDirect

International Journal of Heat and Mass Transfer

journal homepage: www.elsevier.com/locate/ijhmt

An analytical model for the prediction of strip temperatures in hot strip rolling

Jaeboo Kim [a], Junghyeung Lee [b], Sang Moo Hwang [a,*]

[a] Mechanical Engineering Department, Pohang University of Science and Technology, Pohang 790-784, Republic of Korea
[b] Sheet Plate Research Group, POSCO Technical Research Laboratories, Pohang 790-785, Republic of Korea

ARTICLE INFO

Article history:
Received 4 June 2008
Available online 10 December 2008

Keywords:
Finite element method
Heat transfer
Strip temperatures
Finishing mills
Analytical solution

ABSTRACT

In hot strip rolling, sound prediction of the temperature of the strip is vital for achieving the desired finishing mill draft temperature (FDT). In this paper, a precision on-line model for the prediction of temperature distributions along the thickness of the strip in the finishing mill is presented. The model consists of an analytic model for the prediction of temperature distributions in the inter-stand zone, and a semi-analytic model for the prediction of temperature distributions in the bite zone in which thermal boundary conditions as well as heat generation due to deformation are predicted by finite element-based, approximate models. The prediction accuracy of the proposed model is examined through comparison with predictions from a finite element process model.

1. Introduction

In hot strip mills, the thermal history experienced by the strip during processing is one of the most important parameters influencing the product quality, not only because the flow stress is strongly dependent on the temperature but also because the metallurgical properties of product are substantially affected by it. Recently, the increasing demand for a high quality microalloyed steel strip leads to advanced rolling practices such as controlled rolling and, consequently, to the need for precise temperature control.

It is demonstrated during the last two decades that the prediction of the strip temperature can be made far more accurately on the basis of either the finite difference process models [1–10] or the finite element (FE) process models [11–22] than on the basis of the elementary models which inherently involve many simplifying assumptions. However, a precise model such as a FE process model tends to require a large central processing unit time, rendering itself inadequate for on-line calculation.

Presented in this paper is an analytic model for the prediction of temperature distributions in the inter-stand zone of finishing mill. Also presented is a semi-analytic model for the prediction of temperature distributions in the bite zone, in which thermal boundary conditions as well as heat generation due to deformation are predicted by FE-based on-line models. The prediction accuracy of the proposed model is examined though comparison with the predictions from a FE process model.

2. A finite element model

A FE process model applied for the present investigation consist of four basic FE models: a model for the analysis of steady-state thermo-viscoplastic deformation of the strip (Model A), a model for analysis of steady-state heat transfer in the strip (Model B), a model for the analysis of steady-state heat transfer in the work roll (Model C), and a model for analysis of non-steady-state heat transfer in the strip (Model D). As shown in Fig. 1, interaction between the thermal behavior of the work roll and that of strip caused by roll–strip contact, as well as interaction between the thermal behavior of strip and mechanical behavior of strip, are taken into account by iterative solution schemes. Details regarding the process model and its solution accuracy are given in Ref. [21].

It is to be noted that heat transfer in the direction of the roll axis as well as in the direction of strip width are neglected. Also, plane-strain deformation of strip is assumed. Consequently, all basic FE models applied for the present investigation are two dimensional models. The thermal and mechanical boundary conditions adopted for the basic FE models are shown in Fig. 2.

As illustrated in Fig. 3, a sufficiently large number of elements, along with the mesh refinement near the contact zones, are used to construct the roll and strip meshes in order to remove the mesh dependency of the solution accuracy. The element type used is a linear quadrilateral element. 3440 elements are used for the roll, and 2520 elements are used for the strip.

The predicted temperature distributions in the strip as well as in the roll are illustrated in Fig. 4. Clearly seen is the effect of heat transfer from the strip to roll at the roll–strip interface, as well as the effect of heat generation in the strip due to plastic deformation.

* Corresponding author. Tel.: +82 54 279 2173; fax: +82 54 279 5897.
E-mail address: smhwang@postech.ac.kr (S.M. Hwang).

0017-9310/$ - see front matter © 2008 Elsevier Ltd. All rights reserved.
doi:10.1016/j.ijheatmasstransfer.2008.10.013

Nomenclature

f_s	forward slip, $f_s = \frac{V_2 - R\omega}{R\omega}$
H_1	strip inlet thickness
H_2	strip outlet thickness
h_{rw}	heat transfer coefficient due to water cooling, at the roll surface
h_w	heat transfer coefficient due to water cooling, at the strip surface
h_{lub}	heat transfer coefficient at the roll/strip interface
k	thermal conductivity
L	strip length in the inter-stand zone
l_d	contact length at the roll/strip interface
R	roll radius
r	reduction ratio
s	shape factor $s = \frac{2}{2-r}\sqrt{\frac{Rr}{H_1}}$
T_1	strip inlet temperature
T_2	strip exit temperature
T_s	strip temperature at the roll/strip interface
T_R	roll temperature at the roll/strip interface
u^n	normal component of the velocity vector
u_x, u_y	x, y component of the velocity vector
V_s	strip velocity at the roll/strip interface
V_R	roll tangential velocity
V_1	strip inlet velocity at the bite zone
V_2	strip outlet velocity at the bite zone
V_{it}	strip velocity in the inter-stand zone

Greek symbols

$\bar{\varepsilon}$	effective strain
$\dot{\bar{\varepsilon}}$	effective strain rate
Γ_c	roll/strip interface
μ	coefficient of Coulomb friction
ρc_p	heat capacity
Ω	plastic deformation zone(bite zone) in the strip
σ	flow stress
σ_1	back tension, in a stress unit
σ_2	front tension, in a stress unit
σ_n	normal stress
σ_t	tangential stress
ω	roll angular velocity
ξ	penalty constant

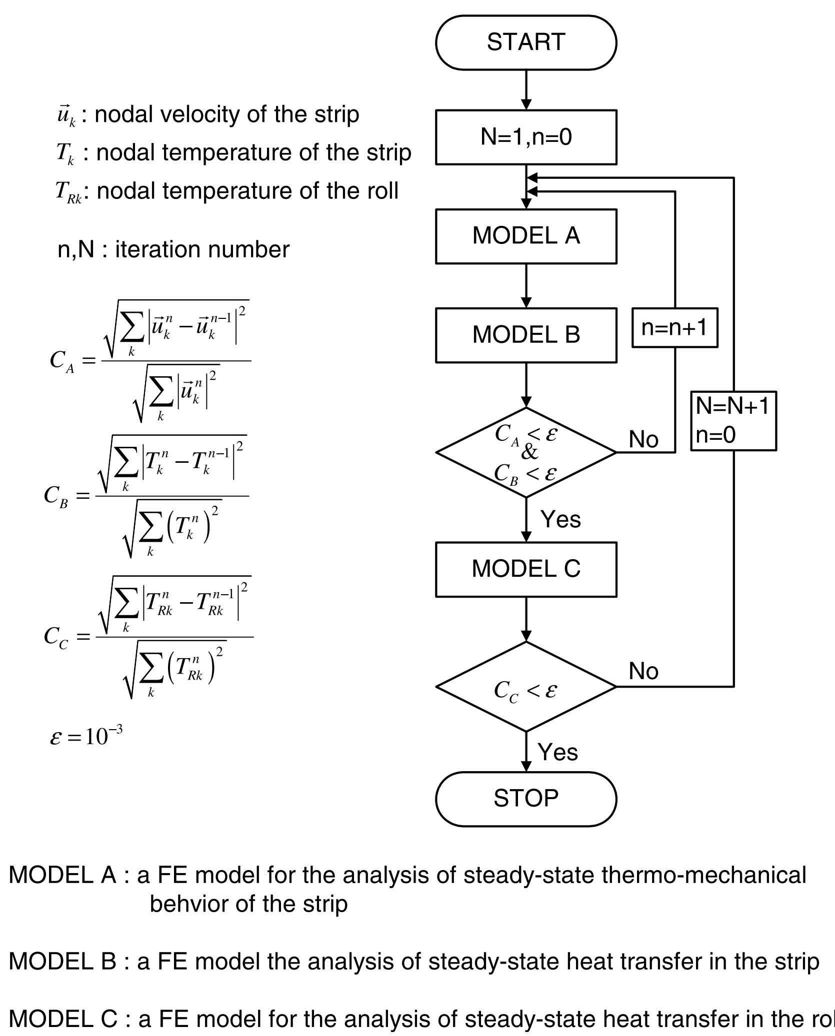

Fig. 1. An integrated FE process model for the analysis of the thermo-mechanical behavior of strip.

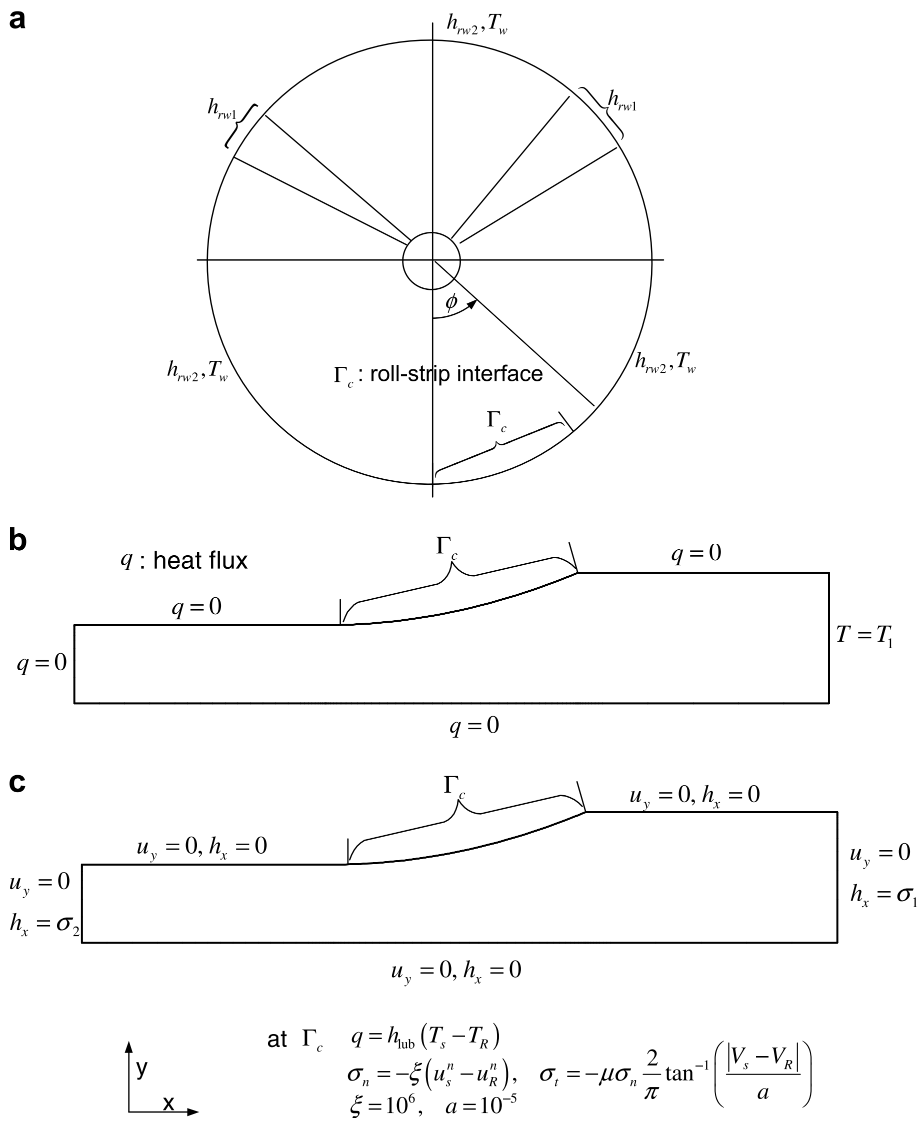

Fig. 2. Boundary conditions for the basic FE models: (a) thermal boundary conditions for the roll, (b) thermal boundary conditions for the strip, and (c) mechanical boundary conditions for the strip.

The process simulation requires approximately 20 min of CPU time of a modern personal computer, which clearly indicates that a FE process model cannot be directly employed as an on-line model, at least not in the near future, considering that the temperature calculations should be carried out in a tiny fraction of a second for on-line process control.

3. An analytic model for the prediction of temperatures in the inter-stand zone

The strip temperatures vary in the inter-stand zone of the hot strip mill where the cooling water is sprayed, mainly due to the convection heat transfer at the strip surface.

Let us define $T_i(y)$ and $T_{i+1}(y)$, the strip temperature distribution at the entry and at the exit of the inter-stand between F_i stand and F_{i+1} stand, respectively, as shown in Fig. 5.

Then the initial boundary value problem to be solved may be given by

heat equation:

$$\frac{\partial}{\partial y}\left(k\frac{\partial T(y,t)}{\partial y}\right) = \rho c_p \frac{\partial T(y,t)}{\partial t} \tag{1}$$

boundary conditions:

$$\frac{\partial T(y,t)}{\partial y} = 0 \quad \text{at } y = 0 \tag{2}$$

$$-k\frac{\partial T(y,t)}{\partial y} = h_w(T(y,t) - T_w) \quad \text{at } y = h \tag{3}$$

initial condition:

$$T(y,0) = T_i(y) \tag{4}$$

The solution, which may be derived from the technique known as the method of separation of variables, is given by

$$T(y,t) = T_w + \sum_{n=1}^{\infty}\left(\frac{4\lambda_n\int_0^h T_i(y)\cdot\cos(\lambda_n y)dy - 4T_w\cdot\sin(\lambda_n h)}{2\lambda_n h + \sin(2\lambda_n h)} \cdot\cos(\lambda_n y)\cdot\exp\left(-\frac{k\cdot\lambda_n^2}{\rho c_p}t\right)\right) \tag{5}$$

where T_w is water temperature, h_w is convection heat transfer coefficient at the strip surface, h is a strip thickness, k is the thermal conductivity of a strip, ρc_p is the heat capacity per unit volume of a strip, and λ_n are obtained by solving

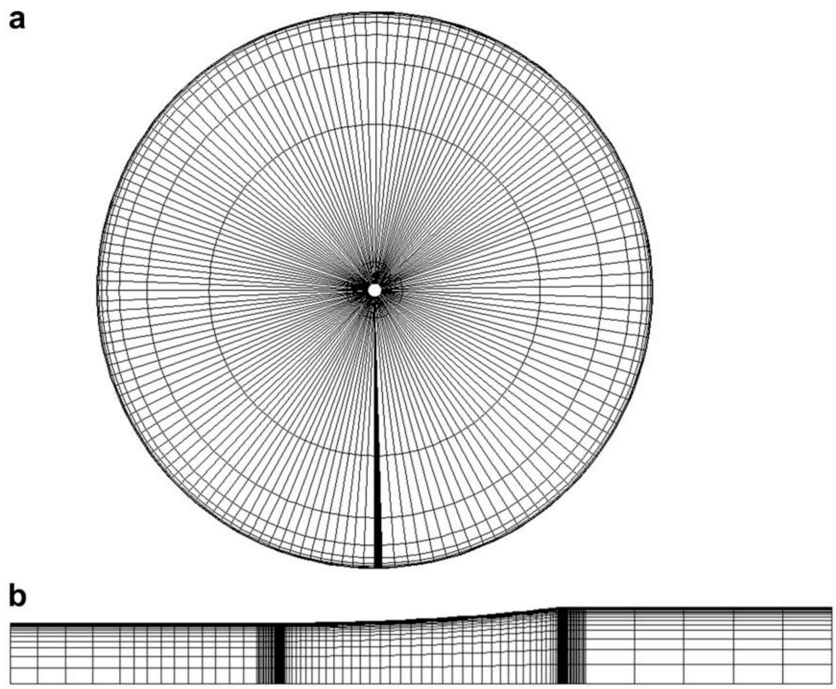

Fig. 3. (a) FE mesh for the roll, (b) FE mesh for the strip.

$$k\lambda_n \sin(\lambda_n h) - h_w \cos(\lambda_n h) = 0 \tag{6}$$

As shown in Fig. 6, the temperature distributions in the inter-stand zone predicted from the proposed model are in excellent agreement with the prediction from FE process model (Model D).

4. A model for the prediction of heat generation due to plastic deformation in the bite zone

Heat generation due to plastic deformation during rolling substantially affects the thermal behavior of strip, and therefore, should be rigorously reflected in predicting the temperature distributions in the bite zone. Due to surface chilling as well as severe shear deformation at the strip surface, heat generation may often become severely non-uniform along the thickness direction.

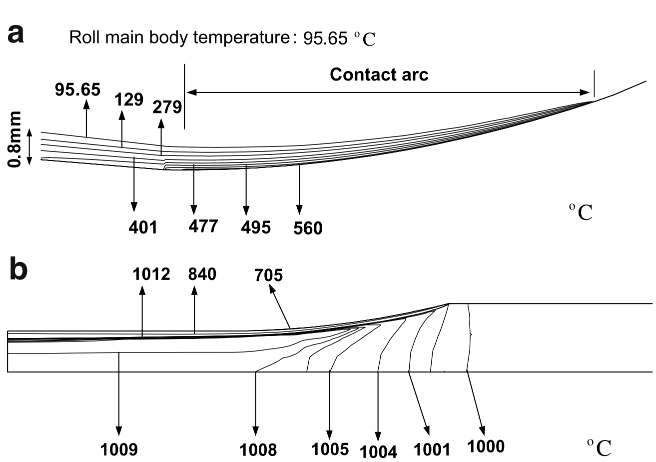

Fig. 4. (a) Temperature distributions in the roll near the bite zone, (b) temperature distributions in the strip at the bite zone, predicted from FE process simulation. Process conditions; carbon pct of the strip material = 0.155, T_1 = 1000 °C, ω = 2.78 rad/s, R = 410 mm, H_1 = 44.52 mm, H_2 = 27.22 mm.

The average heat generation occurring in a particle flowing though the bite zone may approximately given by

$$\dot{q}(y') = \frac{\int_{y'} \bar{\sigma}\,\dot{\bar{\varepsilon}}\,d\Omega}{\int_{y'} d\Omega} \tag{7}$$

where y' denotes the normalized distance from the centerline, with y' = 1 representing the surface, and the integration is performed along the streamline y' = *constant*.

By examining the actual distributions of $\dot{q}(y')$ predicted from FE process simulation, which are illustrated in Figs. 7 and 8, it may be deduced that distribution may be approximated by

$$\frac{\dot{q}(y')}{\dot{q}(1)} = 1 - (1 - A)\frac{\arctan\{a(1 - y')\}}{\arctan a} \tag{8}$$

where

$$A = \frac{\dot{q}(0)}{\dot{q}(1)} \tag{9}$$

Integration of Eq. (8) leads to

$$\frac{\dot{q}_{avg}}{\dot{q}(1)} = 1 - (1 - A)B \tag{10}$$

where

$$\dot{q}_{avg} = \frac{\int_\Omega \bar{\sigma}\,\dot{\bar{\varepsilon}}\,d\Omega}{\int_\Omega d\Omega} = \frac{P_d}{\int_\Omega d\Omega} \tag{11}$$

$$B = \int_0^1 \frac{\arctan\{a(1 - y')\}}{\arctan a}\,dy' \tag{12}$$

It follows that

$$\dot{q}(y') = \frac{\dot{q}_{avg}}{1 - (1 - A)B}\left\{1 - (1 - A)\frac{\arctan\{a(1 - y')\}}{\arctan a}\right\} \tag{13}$$

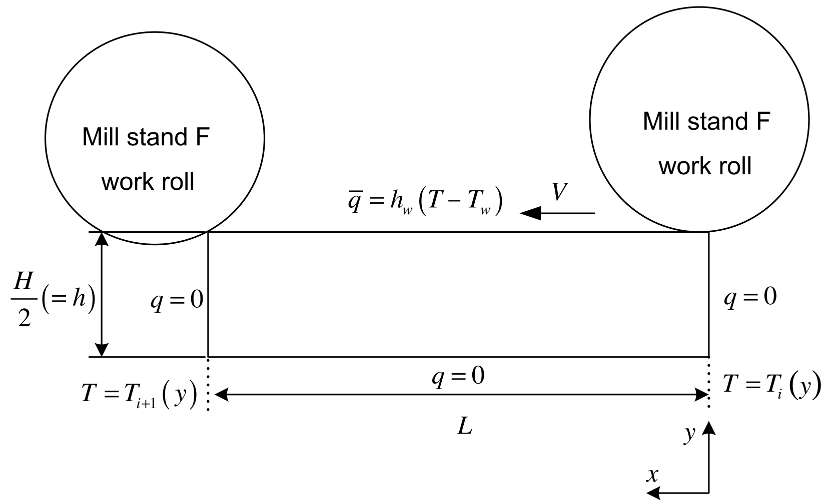

Fig. 5. A definition sketch of an inter-stand zone, inlet = outlet of the bite zone of F_i stand, outlet = inlet of the bite zone of F_{i+1} stand.

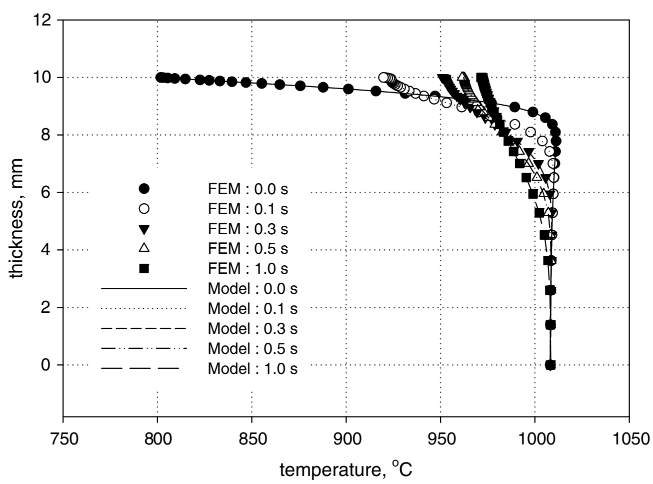

Fig. 6. Temperature distributions along the thickness direction in the inter-stand zone. The temperature distributions at the outlet of the bite zone F_i stand are temperature distributions at the inlet of the inter-stand zone between the stand F_i and the stand F_{i+1}, T_w = 20 °C, h_w = 0.0001 W/mm^2 °C, L = 5800 mm, V = 1800 mm/s.

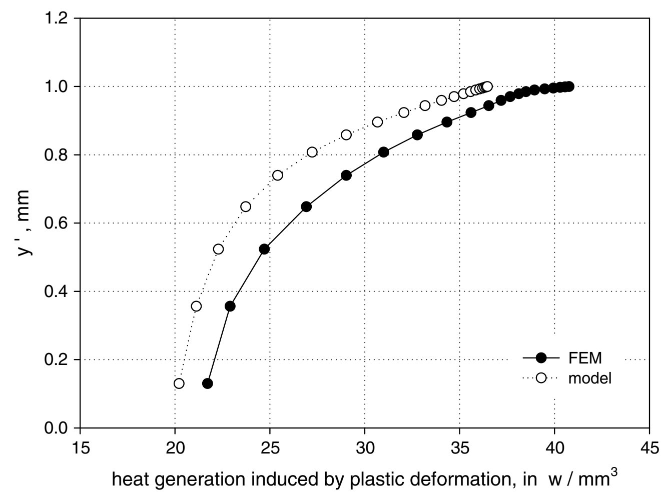

Fig. 8. The average heat generation along the thickness direction in the bite zone of F7 stand. Process conditions are shown in Table 1.

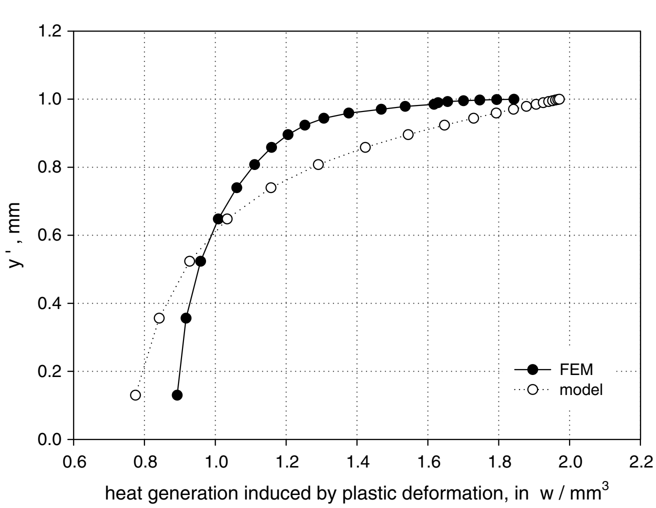

Fig. 7. The average heat generation along the thickness direction in the bite zone of F1 stand. Process conditions are shown in Table 1.

Recently, Kim et al. [24] derived a general dimensionless form that relate the parameters describing the thermo-mechanical behavior of the strip with the process parameters. According to the theory, A may generally be expressed by a function of eight dimensionless variables, or

$$A = f\left(\frac{\omega}{C_2}, \frac{T_1}{C_1}, \mu, s, r, \beta_1, \beta_2, \tilde{\beta}_3\right) \tag{14}$$

where

$$\beta_1 = \frac{\rho c_p V_R}{k} \tag{15}$$

$$\beta_2 = \frac{P'^*}{kT_1} \tag{16}$$

$$\tilde{\beta}_3 = \beta_3 = \frac{P_f - 2P_r}{\overset{*}{P'} + \rho c_p V_R H_1 T_1} \tag{17}$$

$$P'^* = E'_1 V_R H_2 = P'/(1 + f_s) \tag{18}$$

$$P' = V_2 H_2 \frac{2}{\sqrt{3}} \int_{H_2}^{H_1} \frac{\bar{\sigma}(\bar{\varepsilon}, \dot{\bar{\varepsilon}}, T)}{h} dh \tag{19}$$

It is found from a series of FE process simulation that the effect of ω and β_2 are negligible. Assuming that the coefficient of friction μ = 0.3, Eq. (14) may be reduced to a multivariable polynomial form

$$A = f\left(\frac{T_1}{C_1}, s, r, \beta_1, \beta_3\right) = \sum_{i,j,k,l,m} A_{ijklm} s^i r^j T^k \beta_1^l \beta_3^m \tag{20}$$

The coefficients may be found from the least square regression of the data predicted from the FE simulation. The results are given in Tables 2 and 3.

Selecting a = 5, the distribution of $\dot{q}(y')$ the thus predicted are in good agreement with the prediction from the FE process simulation, as shown in Figs. 7 and 8.

5. A semi-analytic model for the prediction of temperatures in the bite zone

The strip temperatures vary in the bite zone, mainly due to heat transfer occurring at the roll and strip interface and also due to heat generation induced by plastic deformation of the strip.Let P_d, P_f, and P_r denote the deformation energy, frictional energy, and the heat loss from the strip to the work roll, respectively, define by

$$P_d = \int_\Omega \bar{\sigma}\,\dot{\bar{\varepsilon}}\,d\Omega \tag{21}$$

$$P_f = \int_{\Gamma_c} \mu\sigma_n |V_s - V_R| d\Gamma \tag{22}$$

$$P_r = \int_{\Gamma_c} h_{\text{lub}}(T_s - T_R) d\Gamma \tag{23}$$

For the prediction of P_d, P_f, and P_r FE-based on-line models proposed by Lee et al. [23] may be used.

Note that heat transfer then average heat flow rate at the roll and strip interface is calculated from

$$q_s = \frac{P_f - 2P_r}{2l_d} \tag{24}$$

The initial boundary value problem associate with heat transfer in the bite zone may be given by heat equation:

$$\frac{\partial}{\partial y}\left(k\frac{\partial T(y,t)}{\partial y}\right) + \dot{q}(y) = \rho c_p \frac{\partial T(y,t)}{\partial t} \tag{25}$$

boundary conditions:

$$\frac{\partial T(y,t)}{\partial y} = 0 \quad \text{at } y = 0 \tag{26}$$

$$k\frac{\partial T(y,t)}{\partial y} = q_s \quad \text{at } y = h \tag{27}$$

where, as shown in Fig. 9, it is assumed that h can be approximated by

$$h = \frac{H_1 + H_2}{4} \tag{28}$$

initial condition:

$$T(y,0) = T_1(y) \tag{29}$$

where $T_1(y)$ denotes inlet temperature distribution.

We may solve the problem by using the method of eigenfunction expansion. The solution procedure is described in detail in Appendix.

The result may be summarized as follows

$$\begin{aligned} T(y,t) = {} & \frac{1}{h}\int_0^h T_1(y)\cdot\phi_0(y)dy + \frac{1}{h\cdot\rho c_p}\left(q_s + \int_0^h \dot{q}(y)dy\right)\cdot t \\ & + \sum_{n=1}^{\infty}\left[\exp\left(-\frac{\lambda_n^2\cdot k}{\rho c_p}t\right)\cdot\left\{a_n(0) + \frac{2\cdot(-1)^n}{h\cdot\rho c_p}\right.\right. \\ & \left.\cdot\int_0^t q_s\cdot\exp\left(\frac{\lambda_n^2\cdot k}{\rho c_p}t\right)dt\right\} + \frac{2}{\lambda_n^2\cdot k\cdot h}\left(1 - \exp\left(-\frac{\lambda_n^2\cdot k}{\rho c_p}t\right)\right) \\ & \left.\cdot\int_0^h \dot{q}(y)\cdot\phi_n(y)dy\right]\phi_n(y) \end{aligned} \tag{30}$$

where $\phi_n(y) = \cos(\lambda_n y)$, $\lambda_n = n\pi/h$ and $a_n(0) = \frac{2}{h}\int_0^h T_1(y)\cdot\phi_n(y)dy$.

The following procedure may then be taken to predict the temperature distribution in the bite zone:

(1) Calculate P_f and P_r from the mathematical expressions derived by Lee et al. [23].
(2) Calculate q_s from Eq. (24).
(3) Calculate P_d from the mathematical expressions derived by Lee et al. [23], and calculate A from Eq. (20).
(4) Calculate heat generation, from Eq. (13).
(5) Calculate the temperature distribution, from Eq. (30).

6. Results and discussion

A finishing mill consists of several mill stands, with its line length being extremely large compared to the strip thickness. Consequently, finite element simulation considering the entire finishing mill as a single analysis domain is impractical in the light of the computational efficiency. An alternative choice would be to divide

Table 1
FE process conditions.

Variables	Unit	F1	F2	F3	F4	F5	F6	F7
H_1	mm	44.52	27.22	16.68	10.82	7.32	5.22	4.02
H_2	mm	27.22	16.68	10.82	7.32	5.22	4.02	3.4
V_R	mm/s	1145	1879	2945	4427	6182	8017	9646
R	mm	410	389	380	340	298	313	322
h_w	W/mm^2 °C	0.000088	0.000132	0.0001584	0.0003	0.0003	0.0003	0.0001584
$\bar{\sigma}$	kN/mm^2	0.155% carbon steel						
T_w	°C	20						
h_{lub}	W/mm^2 °C	0.1						
$\bar{h}_{rw}$	W/mm^2 °C	0.011667						
k_r	W/mm °C	0.027						
ρc_{pr}	J/mm^3 °C	0.004248						
k	W/mm °C	0.03						
ρc_p	J/mm^3 °C	0.00688						
T_0	°C	1000, uniform strip temperature at the inlet F1 bite zone						
L	mm	5800, inter-stand zone length						

Table 2
Mathematical expression for A. $A = f_1(s, r, T, \beta_1, \beta_3) = \sum_{i,j,k,l,m} A_{ijklm} s^i r^j T^k \beta_1^l \beta_3^m$.

i	j	k	l	m	A_{ijklm}	i	j	k	l	m	A_{ijklm}	i	j	k	l	m	A_{ijklm}	i	j	k	l	m	A_{ijklm}
0	0	0	0	0	9.92E+02	0	0	2	0	2	3.54E+O1	0	0	4	0	1	1.69E−07	2	1	0	0	2	1.6E+O5
0	0	0	0	1	1.75E+05	0	0	2	1	1	1.63E−04	0	0	4	1	0	−1.84E−13	2	1	0	1	1	−1.41E−01
0	0	0	1	0	−4.19E−02	0	0	2	2	0	1.89E−12	0	0	5	0	0	−6.20E−13	2	1	0	2	0	−253E−07
0	0	1	0	0	−4.72E+00	0	0	3	0	1	−7.16E−04	0	1	0	1	3	−1.80E+O4	2	1	1	0	1	1.01E+O1
0	1	0	0	0	−4.73E+02	0	0	3	1	0	3.86E−10	0	1	0	2	2	1.94E−02	2	1	1	1	0	−1.79E−05
1	0	0	0	0	−1.27E+02	0	0	4	0	0	3.7E−09	0	1	1	0	3	−152E+05	2	1	2	0	0	3.81E−03
0	0	0	0	2	7.33E+06	0	1	0	0	3	3.2E+07	0	1	1	1	2	2.02E401	2	2	0	0	1	7.26E+02
0	0	0	1	1	7.07E+00	0	1	0	1	2	−5.01E+03	0	1	1	2	1	4.62E−06	2	2	0	1	0	2.0E−03
0	0	0	2	0	7.26E−07	0	1	0	2	1	−9.66E−04	0	1	2	0	2	2.04E402	2	2	1	0	0	3.60E−01
0	0	1	0	1	−7.17E+02	0	1	1	0	2	−1.65E+0J	0	1	2	1	1	3.2E−05	0	0	1	2	3	952E−04
0	0	1	1	0	2.08E−04	0	1	1	1	1	4.11E−02	0	1	2	2	0	−235E−11	0	0	2	1	3	5.10E−02
0	0	2	0	0	8.80E−03	0	1	1	2	0	1.05E−08	0	1	3	0	1	8.7E−03	0	0	2	2	2	3.46E−07
0	1	0	0	1	−3.95E+05	0	1	2	0	1	−7.21E+00	0	1	3	1	0	4.76E−10	0	0	3	0	3	−1.18E+00
0	1	0	1	0	−7.54E−02	0	1	2	1	0	−4.63E−07	0	1	4	0	0	1.95E−08	0	0	3	1	2	−1.19E−05
0	1	1	0	0	−2.36E+00	0	1	3	0	0	−2.70E−0J	0	2	0	0	3	1.06E408	0	0	3	2	1	3.28E−12
0	2	0	0	0	1.05E+04	0	2	0	0	2	−1.45E+07	0	2	0	1	2	3.49E402	0	0	4	0	2	−3.24E−06
1	0	0	0	1	−2.96E+04	0	2	0	1	1	137E+02	0	2	0	2	1	−2.92E−04	0	0	4	1	1	133E−10
1	0	0	1	0	−5.45E−03	0	2	0	2	0	−8.19E−06	0	2	1	0	2	5.62E−*04	0	0	4	2	0	−2.11E−18
1	0	1	0	0	6.07E−01	0	2	1	0	1	−7.01E+03	0	2	1	1	1	−5.47E−01	0	0	5	0	1	3.77E−12
1	1	0	0	0	6.90E+02	0	2	1	1	0	−436E−04	0	2	1	2	0	2.25E−08	0	0	5	1	0	3.3E−17
2	0	0	0	0	5.59E+01	0	2	2	0	0	5.73E−02	0	2	2	0	1	1.26E401	0	1	0	2	3	1.17E−01
0	0	0	0	3	1.33E+08	1	0	0	0	3	−9.66E+0S	0	2	2	1	0	6.80E−07	0	1	1	1	3	6.28E+01
0	0	0	1	2	4.82E+02	1	0	0	1	2	3.4E+02	0	2	3	0	0	−3.05E−05	0	1	1	2	2	−5.52E−05
0	0	0	2	1	8.98E−05	1	0	0	2	1	8.18E−05	1	0	0	1	3	−9.62E+02	0	1	2	0	3	259E+02
0	0	1	0	2	−2.76E+04	1	0	1	0	2	5.14E+03	1	0	0	2	2	237E−03	0	1	2	1	2	−3.04E−02
0	0	1	1	1	−5.73E−02	1	0	1	1	1	−2.S8E−02	1	0	1	0	3	4.05E−HJ4	0	1	2	2	1	−8.02E−09
0	0	1	2	0	−239E−09	1	0	1	2	0	−134E−09	1	0	1	1	2	−1.4E+00	0	1	3	0	2	−753E−02
0	0	2	0	1	1.09E+00	1	0	2	0	1	−7.69E−02	1	0	1	2	1	−3J1E−07	0	1	3	1	1	−137E−07
0	0	2	1	0	−4.04E−07	1	0	2	1	0	8.3E−10	1	0	2	0	2	−2.46E+00	0	1	3	2	0	2.05E−14
0	0	3	0	0	−8.02E−06	1	0	3	0	0	8.74E−07	1	0	2	1	1	4.60E−05	0	1	4	0	1	−4.86E−06
0	1	0	0	2	4.0E+07	1	1	0	0	2	−933E+0S	1	0	2	2	0	3.18E−12	0	1	4	1	0	−2.78E−13
0	1	0	1	1	−2.13E+01	1	1	0	1	1	−1.27E+01	1	0	3	0	1	−4.66E−05	0	1	5	0	0	−5.11E−12
0	1	0	2	0	−1.21E−06	1	1	0	2	0	1.86E−07	1	0	3	1	0	−3.90E−11	0	2	0	1	3	4.44E+03
0	1	1	0	1	2.83E+03	1	1	1	0	1	−6.28E+02	1	0	4	0	0	−3.16E−10	0	2	0	2	2	−1.72E−03
0	1	1	1	0	2.74E−04	1	1	1	1	0	8.15E−05	1	1	0	0	3	−8.19E+05	0	2	1	0	3	−2.00E+05
0	1	2	0	0	1.4E−02	1	1	2	0	0	−2.66E−03	1	1	0	1	2	−4.88E+01	0	2	1	1	2	−1.03E+00
0	2	0	0	1	1.2E+06	1	2	0	0	1	−3.73E+03	1	1	0	2	1	−1.19E−04	0	2	1	2	1	8.15E−07
0	2	0	1	0	1.27E−01	1	2	0	1	0	4.70E−02	1	1	1	0	2	3.9E404	0	2	2	0	2	−7.70E+01
0	2	1	0	0	−4.12E+01	1	2	1	0	0	1.63E+01	1	1	1	1	1	5.85E−02	0	2	2	1	1	8.15E−04
1	0	0	0	2	−1.74E+06	2	0	0	0	2	3.10E+05	1	1	1	2	0	−1.83E−09	0	2	2	2	0	−2.01E−11
1	0	0	1	1	6.07E+00	2	0	0	1	1	5.76E−01	1	1	2	0	1	138E400	0	2	3	0	1	−1.10E−02
1	0	0	2	0	l.75E−07	2	0	0	2	0	6.17E−08	1	1	2	1	0	−6.46E−08	0	2	3	1	0	−6.45E−10
1	0	1	0	1	9.62E+01	2	0	1	0	1	−3.74E+01	1	1	3	0	0	8.11E−06	0	2	4	0	0	1.4E−09
1	0	1	1	0	1.50E−05	2	0	1	1	0	−1.86E−0J	1	2	0	0	2	1.46E406	1	0	0	2	3	3.42E−02
1	0	2	0	0	−1.08E−03	2	0	2	0	0	5.43E−04	1	2	0	1	1	−1.88E+00	1	0	1	1	3	2.68E+00
1	1	0	0	1	1.04E+05	2	1	0	0	1	−8.87E+02	1	2	0	2	0	3.28E−06	1	0	1	2	2	−9.21E−06
1	1	0	1	0	−2.08E−02	2	1	0	1	0	5.12E−03	1	2	1	0	1	1.5E−HJ3	1	0	2	0	3	−6.18E+01
1	1	1	0	0	−1.21E+00	2	1	1	0	0	−1.65E+00	1	2	1	1	0	−2.72E−04	1	0	2	1	2	2.47E−03
1	2	0	0	0	−3.85E+03	2	2	0	0	0	−9.15E+01	1	2	2	0	0	−2.9E−02	1	0	2	2	1	5.49E−10
2	0	0	0	1	7.94E+03	0	0	0	2	3	−4.61E−01	2	0	0	0	3	7.05E404	1	0	3	0	2	−5.80E−03
2	0	0	1	0	392E−03	0	0	1	1	3	−3J64E+01	2	0	0	1	2	−3.15E+00	1	0	3	1	1	−3.84E−08
2	0	1	0	0	−2.78E−01	0	0	1	2	2	−2.11E−04	2	0	0	2	1	1.24E−05	1	0	3	2	0	−3.18E−15
2	1	0	0	0	2.84E+02	0	0	2	0	3	1.24E+03	2	0	1	0	2	−1.28E+03	1	0	4	0	1	8.6SE−08
0	0	0	1	3	9.73E+03	0	0	2	1	2	9.23E−03	2	0	1	1	1	−2.78E−03	1	0	4	1	0	4.25E−14
0	0	0	2	2	4.72E−02	0	0	2	2	1	−1.70E−09	2	0	1	2	0	−7.29E−11	1	0	5	0	0	3.70E−14
0	0	1	0	3	−6.43E+05	0	0	3	0	2	−1.47E−02	2	0	2	0	1	6.89E−02	1	1	0	1	3	−2.28E+02
0	0	1	1	2	−3.43E+00	0	0	3	1	1	−2.14E−07	2	0	2	1	0	3.19E−08	1	1	0	2	2	2.3E−03
0	0	1	2	1	1.51E−07	0	0	3	2	0	12 1E−15	2	0	3	0	0	−5.21E−07	1	1	1	0	3	1.20E+04

the finishing mill into several sub zones. As shown in Fig. 10a, each zone may be classified into one of the following four types: the first zone, which represents a region located in front of the first mill stand, the last zone, which represents a region located between the last mill stand and somewhere in front of the run-out-table for water cooling, inter-stand zone, and a mill stand zone occupied by the roll–strip system. As shown in Fig. 10b, simulation may be preformed for each zone in sequence, starting from first zone and employing the temperatures predicted at the current zone as the initial conditions for next simulation, until simulation for the last zone.The inter-stand zone model and bite zone model are then combined into an on-line model for prediction of temperature distributions at any given location in the finishing mill. Here, $\Delta t_1 = L/V_{it}$ is inter-stand zone passing time which is function of known process variables, inter-stand zone length and strip velocity in the inter-stand zone. $\Delta t_2 = l_d/V_R$ is bite zone passing time which is function of known process variables, contact length at the roll/strip interface and roll tangential velocity. The predictions are in excellent agreement with FE predictions, as shown in Figs. 11 and 12, indicating that the assumptions made for the derivation of the inter-stand zone model as well as for the derivation of the bite zone model are valid. Also noted is that the average temperature of strip may possibly be seriously underestimated if the measurement of the surface temperature is made near the roll exit,

Table 3
Mathematical expression for A (continued). $A = f_1(s, r, T, \beta_1, \beta_3) = \sum_{i,j,k,l,m} A_{ijklm} s^i r^j T^k \beta_1^l \beta_3^m$.

i	j	k	l	m	A_{ijklm}	i	j	k	l	m	A_{ijklm}	i	j	k	l	m	A_{ijklm}	i	j	k	l	m	A_{ijklm}
1	1	1	1	2	2.61E−01	0	1	4	1	1	1.1 IE−10	2	0	4	0	1	2.75E−08	1	1	2	1	3	−1J84E−04
1	1	1	2	1	3.85E−07	0	1	4	2	0	−6J86E−18	2	0	4	1	0	5.46E−15	1	1	2	2	2	1J60E−09
1	1	2	0	2	−5.14E+01	0	1	5	0	1	106E−09	2	0	5	0	0	−459E−14	1	1	3	0	3	6J22E−03
1	1	2	1	1	−9.79E−05	0	1	5	1	0	6.69E−17	2	1	0	1	3	−524E+00	1	1	3	1	2	1.45E−07
1	1	2	2	0	3.72E−12	0	2	0	2	3	254E−03	2	1	0	2	2	−2.70E−04	1	1	3	2	1	1J26E−13
1	1	3	0	1	−1.41E−03	0	2	1	1	3	−899E+00	2	1	1	0	3	−1.13E+03	1	1	4	0	2	−7.78E−06
1	1	3	1	0	−6.99E−11	0	2	1	2	2	433E−06	2	1	1	1	2	4.62E−04	1	1	4	1	1	−lS0E−11
1	1	4	0	0	−6.84E−09	0	2	2	0	3	109E+02	2	1	1	2	1	−9.63E−09	1	1	4	2	0	5J07E−19
1	2	0	0	3	−2.57E+07	0	2	2	1	2	102E−03	2	1	2	0	2	338E−01	1	1	5	0	1	−136E−10
1	2	0	1	2	−6.76E+01	0	2	2	2	1	−783E−10	2	1	2	1	1	−6.02E−07	1	1	5	1	0	−3.73E−17
1	2	0	2	1	−1.29E−05	0	2	3	0	2	450E−02	2	1	2	2	0	−1.13E−12	1	2	0	2	3	1.16E−02
1	2	1	0	2	−4.46E+03	0	2	3	1	1	−537E−07	2	1	3	0	1	157E−05	1	2	1	1	3	−7.41E−02
1	2	1	1	1	4.49E−03	0	2	3	2	0	6.16E−15	2	1	3	1	0	−9.78E−12	1	2	1	2	2	−7S2E−07
1	2	1	2	0	−8.54E−09	0	2	4	0	1	4.62E−06	2	1	4	0	0	238E−09	1	2	2	0	3	−lJGE+0l
1	2	2	0	1	−238E+00	0	2	4	1	0	356E−13	2	2	0	0	3	105E+06	1	2	2	1	2	−430E−05
1	2	2	1	0	5.02E−07	0	2	5	0	0	2.41E−12	2	2	0	1	2	3.46E+00	1	2	2	2	1	−1J22E−11
1	2	3	0	0	1.86E−05	1	0	1	2	3	−567E−05	2	2	0	2	1	801E−07	1	2	3	0	2	−1.12E−03
2	0	0	1	3	6.78E+00	1	0	2	1	3	−2.43E−03	2	2	1	0	2	2.43E+02	1	2	3	1	1	1J04E−09
2	0	0	2	2	528E−05	1	0	2	2	2	108E−08	2	2	1	1	1	17E−04	1	2	3	2	0	−1JS0E−15
2	0	1	0	3	−433E+02	1	0	3	0	3	402E−02	2	2	1	2	0	421E−10	1	2	4	0	1	−3S4E−07
2	0	1	1	2	8.45E−03	1	0	3	1	2	−1.75E−06	2	2	2	0	1	904E−03	1	2	4	1	0	9.75E−14
2	0	1	2	1	−392E−08	1	0	3	2	1	−3.79E−13	2	2	2	1	0	657E−10	1	2	5	0	0	3S3E−13
2	0	2	0	2	196E+00	1	0	4	0	2	7.11E−06	2	2	3	0	0	4.11E−07	2	0	1	2	3	2.44E−07
2	0	2	1	1	4.86E−06	1	0	4	1	1	156E−11	0	0	3	2	3	958E−11	2	0	2	1	3	8.74E−06
2	0	2	2	0	−1.72E−13	1	0	4	2	0	128E−18	0	0	4	1	3	72E−09	2	0	2	2	2	−lSlE−11
2	0	3	0	1	−6.21E−05	1	0	5	0	1	−298E−11	0	0	4	2	2	65E−14	2	0	3	0	3	−3J23E−04
2	0	3	1	0	−230E−11	1	0	5	1	0	−139E−17	0	0	5	0	3	−1.05E−07	2	0	3	1	2	2.18E−09
2	0	4	0	0	2.46E−10	1	1	0	2	3	−2.19E−02	0	0	5	1	2	−1.79E−12	2	0	3	2	1	−1.49E−14
2	1	0	0	3	3.65E+05	1	1	1	1	3	453E−01	0	0	5	2	1	6.77E−19	2	0	4	0	2	3J26E−07
2	1	0	1	2	−1.15E+00	1	1	1	2	2	−357E−06	0	1	2	2	3	627E−08	2	0	4	1	1	1 J0 IE−12
2	1	0	2	1	3.08E−06	1	1	2	0	3	−1.70E+01	0	1	3	1	3	23E−05	2	0	4	2	0	−1J29E−19
2	1	1	0	2	−4.13E+02	1	1	2	1	2	−357E−04	0	1	3	2	2	−1.49E−11	2	0	5	0	1	−4.77E−12
2	1	1	1	1	4.96E−04	1	1	2	2	1	−383E−10	0	1	4	0	3	3.14E−05	2	0	5	1	0	3J88E−19
2	1	1	2	0	1.01E−09	1	1	3	0	2	326E−02	0	1	4	1	2	−5.08E−09	2	1	0	2	3	−5J87E−04
2	1	2	0	1	−234E−02	1	1	3	1	1	7.12E−08	0	1	4	2	1	−153E−15	2	1	1	1	3	1S0E−03
2	1	2	1	0	2.14E−08	1	1	3	2	0	−253E−15	0	1	5	0	2	19E−08	2	1	1	2	2	1.70E−07
2	1	3	0	0	−430E−06	1	1	4	0	1	685E−07	0	1	5	1	1	−2 PIE−14	2	1	2	0	3	7J23E−01
2	2	0	0	2	−1.01E+05	1	1	4	1	0	1.1 IE−13	0	1	5	2	0	455E−22	2	1	2	1	2	6S2E−07
2	2	0	1	1	−5.44E−02	1	1	5	0	0	191E−12	0	2	1	2	3	−32E−05	2	1	2	2	1	4S9E−12
2	2	0	2	0	−2.01E−07	1	2	0	1	3	286E+01	0	2	2	1	3	40E−03	2	1	3	0	2	−836E−05
2	2	1	0	1	−538E+00	1	2	0	2	2	−2.73E−04	0	2	2	2	2	−929E−10	2	1	3	1	1	2.46E−10
2	2	1	1	0	−4.11E−06	1	2	1	0	3	401E+04	0	2	3	0	3	−122E−02	2	1	3	2	0	4.10E−16
2	2	2	0	0	−5.62E−04	1	2	1	1	2	1.13E−01	0	2	3	1	2	−3.45E−07	2	1	4	0	1	−5S5E−09
0	0	2	2	3	−6.27E−07	1	2	1	2	1	100E−08	0	2	3	2	1	2.45E−13	2	1	4	1	0	120E−15
0	0	3	1	3	−3.19E−05	1	2	2	0	2	405E+00	0	2	4	0	2	−92E−06	2	1	5	0	0	−5.16E−13
0	0	3	2	2	−2.48E−10	1	2	2	1	1	−3.61E−06	0	2	4	1	1	132E−10	2	2	0	1	3	1.79E400
0	0	4	0	3	555E−04	1	2	2	2	0	658E−12	0	2	4	2	0	−2.15E−19	2	2	0	2	2	1.76E−04
0	0	4	1	2	7.41E−09	1	2	3	0	1	160E−03	0	2	5	0	1	−7.44E−10	2	2	1	0	3	−9J21E+02
0	0	4	2	1	−2.49E−15	1	2	3	1	0	−3.74E−10	0	2	5	1	0	−825E−17	2	2	1	1	2	−3J85E−03
0	0	5	0	2	2.74E−09	1	2	4	0	0	−5.57E−09	1	0	2	2	3	224E−08	2	2	1	2	1	1J63E−09
0	0	5	1	1	−3.16E−14	2	0	0	2	3	−156E−04	1	0	3	1	3	7.10E−07	2	2	2	0	2	−135E−01
0	0	5	2	0	688E−22	2	0	1	1	3	−1.53E−02	1	0	3	2	2	−4.02E−12	2	2	2	1	1	−1.15E−07
0	1	1	2	3	−1.78E−04	2	0	1	2	2	−200E−08	1	0	4	0	3	−933E−06	2	2	2	2	0	−2 J0SE−13
0	1	2	1	3	−7J02E−02	2	0	2	0	3	691E−01	1	0	4	1	2	48E−10	2	2	3	0	1	−4J26E−06
0	1	2	2	2	497E−08	2	0	2	1	2	−750E−06	1	0	4	2	1	9.79E−17	2	2	3	1	0	8J24E−13
0	1	3	0	3	−1.74E−01	2	0	2	2	1	420E−11	1	0	5	0	2	−225E−09	2	2	4	0	0	−1.17E−10
0	1	3	1	2	203E−05	2	0	3	0	2	−132E−03	1	0	5	1	1	−2.44E−15						
0	1	3	2	1	598E−12	2	0	3	1	1	−3j67E−09	1	0	5	2	0	−125E−22						
0	1	4	0	2	−2.12E−05	2	0	3	2	0	3.14E−16	1	1	1	2	3	209E−05						

and that the temperatures become almost uniform at the region away from F7stand, after rolling.

7. Concluding remarks

The model presented in this paper may serve as an effective tool for the precise control of production speed and pressure of water sprayed in the inter-stand zone, to achieve the desired finishing mill draft temperature (FDT). The model may also serve as a sound basis for exactly deducing the temperature distributions and the average temperature of the strip from the measurement of the strip surface temperature made in the production line, which is vital for enhancing the predicting accuracy of the models for predicting the roll force and roll power, as well as those for predicting the metallurgical behavior of the strip.

Appendix A

Let us consider a homogeneous boundary value problem,

$$\frac{d^2\phi_n}{d^2y} + \lambda_n^2\phi_n = 0 \tag{A1}$$

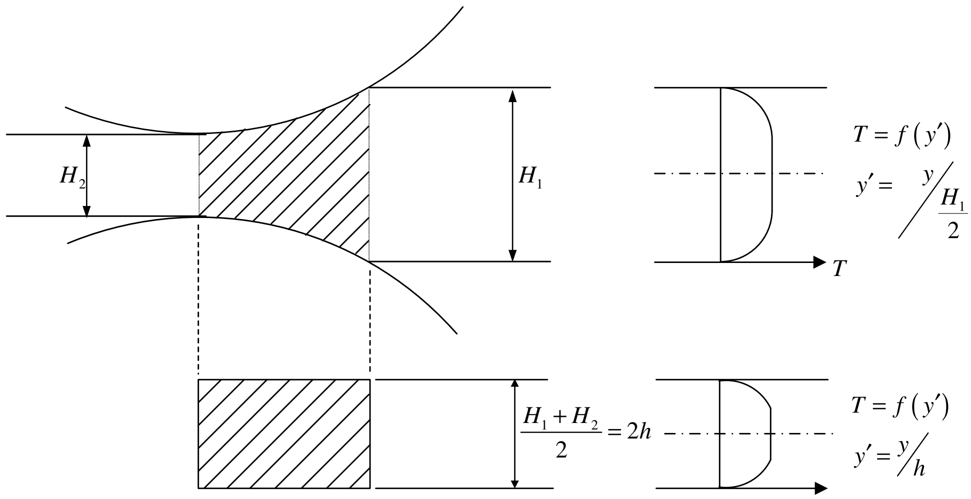

Fig. 9. Approximation of bite zone and temperature distributions at the inlet.

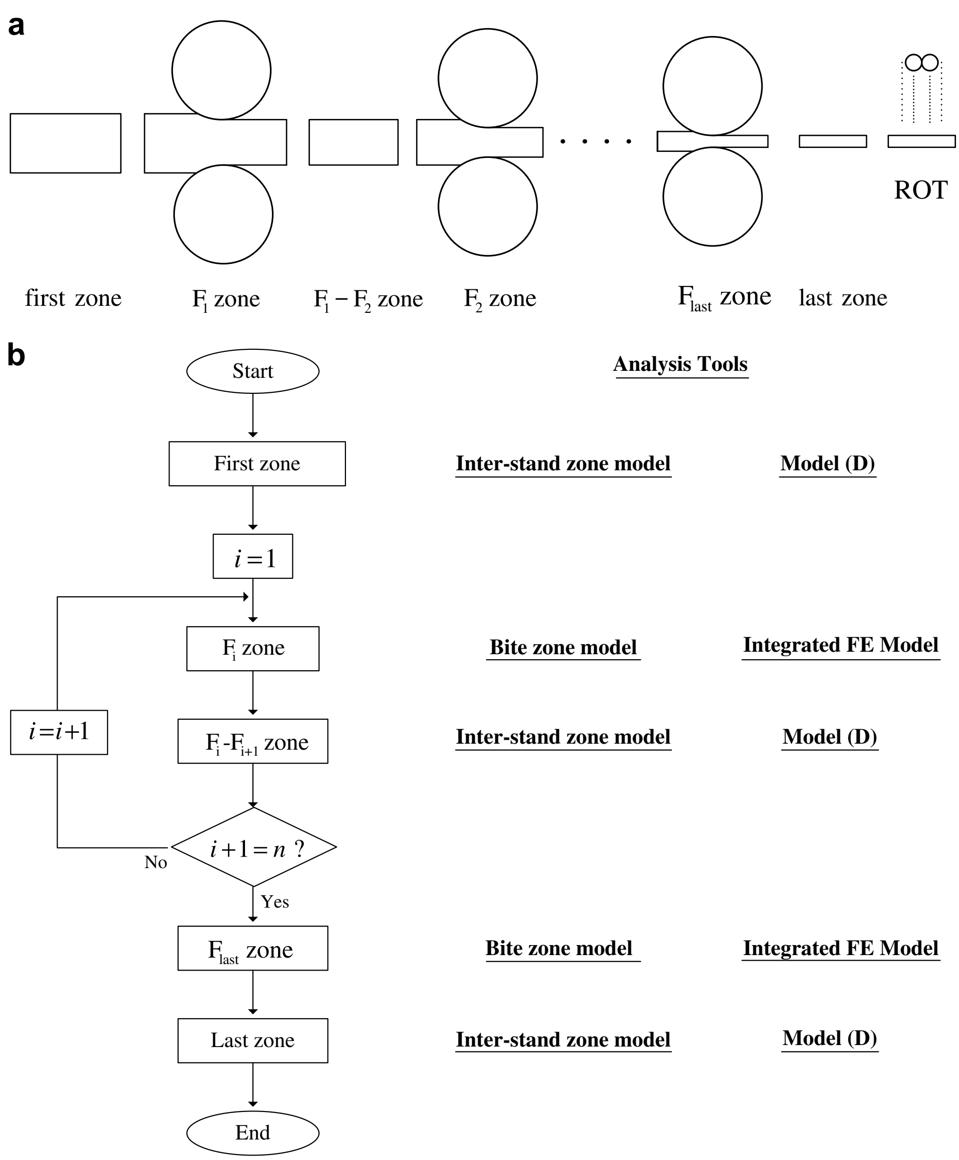

Fig. 10. (a) Division of a finishing mill into several sub zones, (b) Computational procedure.

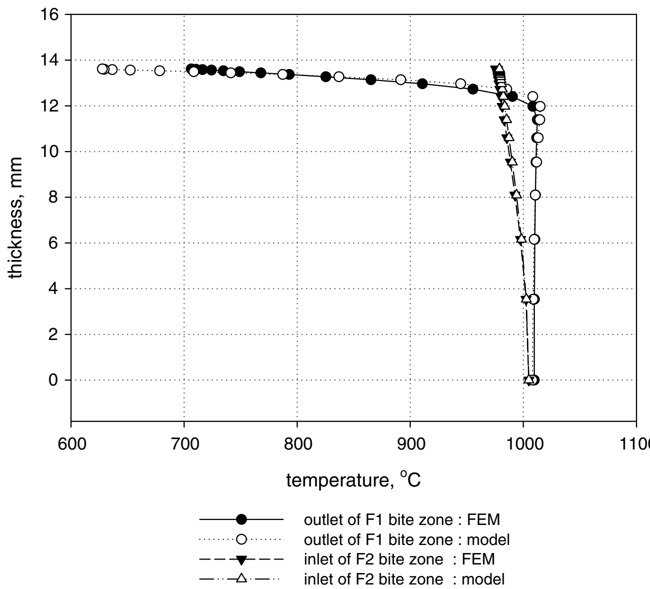

Fig. 11. Temperature distributions along the thickness direction in the finishing mills at the outlet of the bite zone of F1 stand and at the inlet of the bite zone of F2 stand. Process conditions are shown in Table 1.

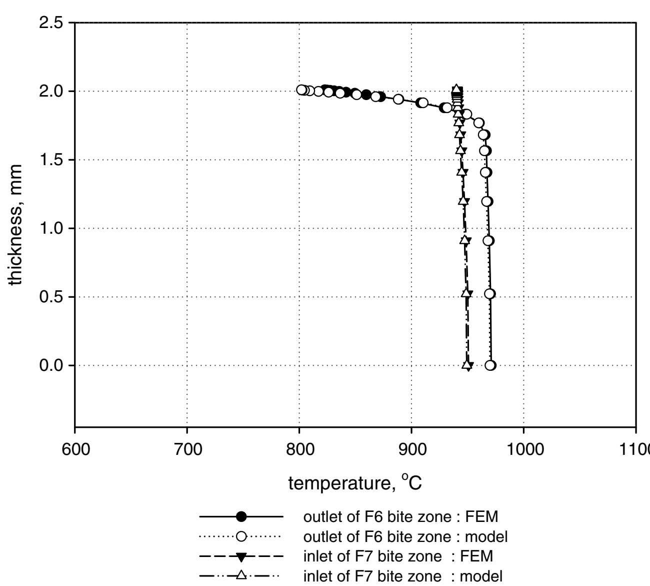

Fig. 12. Temperature distributions along the thickness direction in the finishing mills at the outlet of the bite zone of F6 stand and at the inlet of the bite zone of F7 stand. Process conditions are shown in Table 1.

$$\frac{d\phi_n(0)}{dy} = 0 \tag{A2}$$

$$\frac{d\phi_n(h)}{dy} = 0 \tag{A3}$$

The eigen functions are given by

$$\phi_n(y) = \cos(\lambda_n y), \quad \lambda_n = n\pi/h \tag{A4}$$

Any piecewise smooth function can be expand in terms of these eigen functions, or

$$T(y,t) = \sum_{n=0}^{\infty} a_n(t) \cdot \phi_n(y) \tag{A5}$$

It follows that

$$\frac{\partial T(y,t)}{\partial t} = \sum_{n=0}^{\infty} \frac{da_n(t)}{dt} \cdot \phi_n(y) \tag{A6}$$

$$a_n(t) = \frac{\int_0^h T(y,t) \cdot \phi_n(y)dy}{\int_0^h \phi_n^2(y)dy} \tag{A7}$$

From (25) and (A6), it may be shown that

$$\frac{da_n(t)}{dt} = \frac{\int_0^h \left[\frac{k}{\rho c_p}\frac{\partial^2 T(y,t)}{\partial y^2} + \frac{1}{\rho c_p}\dot{q}(y)\right] \cdot \phi_n(y)dy}{\int_0^h \phi_n^2(y)dy} \tag{A8}$$

In order to derive an expression for $a_n(t)$, let us consider Green's formula

$$\int_0^h \left[u \cdot \frac{\partial^2 v}{\partial y^2} - v \cdot \frac{\partial^2 u}{\partial y^2}\right]dy = \left(u\frac{dv}{dy} - v\frac{du}{dy}\right)\Big|_0^h \tag{A9}$$

where $u = T(y, t)$, $v = \phi_n(y)$.

The left-hand side of (A9) is reduced to

$$\int_0^h \left[u \cdot \frac{\partial^2 v}{\partial y^2} - v \cdot \frac{\partial^2 u}{\partial y^2}\right]dy = -\lambda_n^2 \int_0^h T(y,t) \cdot \phi_n(y)dy - \int_0^h \frac{\partial^2 T(y,t)}{\partial y^2} \cdot \phi_n(y)dy \tag{A10}$$

And the right-hand side of (A9) is reduced to

$$\left(u\frac{dv}{dy} - v\frac{du}{dy}\right)\Big|_0^h = (-1)^{n+1} \cdot \frac{q_s}{k} \tag{A11}$$

Thus, from (A8)

$$\int_0^h \frac{\partial^2 T(y,t)}{\partial y^2} \cdot \phi_n(y)dy = -\lambda_n^2 \int_0^h T(y,t) \cdot \phi_n(y)dy + (-1)^n \cdot \frac{q_s}{k} \tag{A12}$$

Equation (A8) then becomes

Case 1: $n = 0$

$$\frac{da_0(t)}{dt} = \frac{1}{h \cdot \rho c_p}\left(q_s + \int_0^h \dot{q}(y)dy\right) \tag{A13}$$

Case2: $n \neq 0$

$$\frac{da_n(t)}{dt} = -\frac{\lambda_n^2 \cdot k}{\rho c_p} a_n(t) + \frac{2}{h \cdot \rho c_p}\left((-1)^n q_s + \int_0^h \dot{q}(y) \cdot \phi_n(y)dy\right) \tag{A14}$$

From (A13), we obtain

$$a_0(t) = a_0(0) + \frac{1}{h \cdot \rho c_p}\left(q_s + \int_0^h \dot{q}(y)dy\right) \cdot t \tag{A15}$$

$$\text{where from (A7) } a_0(0) = \frac{1}{h}\int_0^h T_1(y) \cdot \phi_0(y)dy \tag{A16}$$

Equation (A14) may be solved by introducing the integrating factor $\exp\left(\lambda_n^2 \frac{k}{\rho c_p} t\right)$. The result may be summarized as follows.

$$a_n(t) = \exp\left(-\lambda_n^2 \frac{k}{\rho c_p} t\right) \cdot \left\{a_n(0) + \frac{2 \cdot (-1)^n}{h \cdot \rho c_p} \cdot \int_0^t q_s \cdot \exp\left(\lambda_n^2 \frac{k}{\rho c_p} t\right)dt\right\} + \frac{2}{\lambda_n^2 \cdot k \cdot h}\left(1 - \exp\left(-\lambda_n^2 \frac{k}{\rho c_p} t\right)\right) \cdot \int_0^h \dot{q}(y) \cdot \phi_n(y)dy \tag{A17}$$

$$\text{where from (A7) } a_n(0) = \frac{2}{h}\int_0^h T_1(y) \cdot \phi_n(y)dy \tag{A18}$$

References

[1] D.M. Parke, J.L.L. Baker, Temperature effects of cooling work rolls, Iron Steel Eng. 49 (1972) 83–88.
[2] Y. Sekimoto, K. Tanaka, K. Nakajima, T. Kawanami, Effects of rolling condition on the surface temperature of work roll in hot strip mill, Trans. Iron Steel Inst. Jpn. 16 (1976) 551–560.
[3] G.D. Lahoti, S.N. Shah, T. Altan, Computer aided analysis of the deformations and temperature in strip rolling, ASME J. Eng. Ind. 100 (1978) 159–166.
[4] A. Ohnuki, K. Nakajima, Work roll surface deterioration in hot strip rolling, in: Proceedings of the Fourth International Conference on Production Engineering, Tokyo, 1980, pp. 1041–1046.
[5] A.A. Tseng, Numerical heat transfer analysis of strip rolling, ASME J. Heat Transfer 106 (1984) 512–517.
[6] C. Devadas, I.V. Samarasekera, Heat transfer during hot rolling of steel strip, Ironmaking Steelmaking 13 (1986) 311–321.
[7] A. Laasraoui, J.J. Jonas, Prediction of temperature distribution, flow stress and microstructure during the multipass hot rolling of steel plate and strip, Iron Steel Inst. Jpn. Int. 31 (1991) 95–105.
[8] H. Yoshida, A. Yorifuji, S. Koseki, M. Saeki, Integrated mathematical simulation of temperatures, rolling loads and metallurgical properties in hot strip mills, Iron Steel Inst. Jpn. Int. 31 (1991) 571–576.
[9] B.K. Chen, P.F. Thomson, S.K. Choi, Temperature distribution in the roll-gap during flat rolling, J. Mater. Proc. Technol. 30 (1992) 115–130.
[10] W.C. Chen, I.V. Samarasekera, E.B. Hawbolt, Fundamental phenomena governing heat transfer during rolling, Metallurg. Trans. 24A (1993) 1307–1320.
[11] O.C. Zienkiewicz, E. Onate, J.C. Heinrich, General formulation for coupled thermal flow of metals using finite elements, Int. J. Num. Meth. Eng. 11 (1981) 1497–1514.
[12] J.H. Beynon, P.R. Brown, S.I. Mizban, R.S. Ponter, C.M. Sellars, Inclusion of metallurgical development in the modelling of industrial hot rolling of metals, in: Proceedings of the NUMIFORM ’86, Gothenburg, Sweden, 1986, pp. 213–218.
[13] J.H. Beynon, A.R.S. Ponter, C.M. Cellars, in: J.L. Chenot, E. Onate (Eds.), Modelling of Metal Forming Processes, Kluwer Academic Publishers, Dordrecht, Netherlands, 1998, pp. 321–328.
[14] M. Pietrzyk, J.G. Lenard, Thermal–Mechanical Modeling of the Flat Rolling Processes, Springer-Verlag, Berlin, 1991.
[15] K. Yamada, S. Ogawa, S. Hamauzu, Two-dimensional thermo-mechanical analysis of flat rolling using rigid-plastic finite element method iron steel, Inst. Jpn. Int. 31 (1991) 566–570.
[16] A. Kumar, I.V. Samarasekera, E.B. Hawbolt, Roll-bite deformation during the hot rolling of steel strip, J. Mater. Process. Technol. 30 (1992) 91–114.
[17] M. Pietrzyk, Z. Kedzierski, J.G. Lenard, Finite element simulation of mechanical, thermal, and structural phenomena in the hot rolling process, in: Proceedings of the NUMIFORM’92, Valbonne, France, 1992, pp. 749–754.
[18] S. Nanba, M. Kitamura, M. Shimada, M. Katsumada, T. Inoue, H. Imamura, Y. Maeda, S. Hattori, Prediction of microstructure distribution in the through-thickness direction during and after hot rolling in the carbon steels, Iron Steel Inst. Jpn. Int. 32 (1992) 377–386.
[19] S.M. Hwang, M.S. Joun, Y.H. Kang, Finite element analysis of temperatures, metal flow, and roll pressure in hot strip rolling, ASME J. Eng. Ind. 115 (1993) 290–298.
[20] M. Kiuchi, J. Yanagimoto, E. Wakamatsu, Thermal analysis of hot plate/sheet rolling, in: Proceedings of the Seventh International Steel Rolling Conference, Chiba, Japan, 1998, pp. 227–232.
[21] C.G. Sun, C.S. Yun, J.S. Chung, S.M. Hwang, Investigation of thermo-mechanical behavior of a work roll and of roll life in hot strip rolling, Met. Mater. Trans. 29A (1998) 2407–2423.
[22] S.M. Hwang, C.G. Sun, S.R. Ryoo, W.J. Kwak, An integrated FE process model for precision analysis of thermo-mechanical behaviors of rolls and strip in the hot strip rolling, Comput. Methods Appl. Mech. Eng. 191 (2002) 4015–4033.
[23] J.H. Lee, W.J. Kwak, C.G. Sun, K.H. Ko, S.M. Hwang, Precision online model for prediction of strip temperature in hot strip rolling, Ironmaking Steelmaking 31 (2004) 153–168.
[24] S.H. Kim, J.H. Lee, W.J. Kwak, S.M. Hwang, Dimensional analysis of hot strip rolling for on-line prediction of thermo-mechanical behavior of roll–strip system, Iron Steel Inst. Jpn. Int. 45 (2005) 199–208.